Sugio, S., Oka, K., Ohishi, H., Tomita, K., & Saenger, W. (1985b) *FEBS Lett. 183*, 115–118.

Sugio, S., Amisaki, T., Ohishi, H., & Tomita, K. (1988) *J. Biochem. 103*, 354–366.

Wlodawer, A., Miller, M., & Sjölin, L. (1983) *Proc. Natl. Acad. Sci. U.S.A. 80*, 3628–3631.

Yu, H.-A., Karplus, M., & Hendrickson, W. A. (1985) *Acta Crystallogr. B41*, 191–201.

Structural Analysis of Specificity: α-Lytic Protease Complexes with Analogues of Reaction Intermediates[†,‡]

Roger Bone,[§] Dan Frank,[§] Charles A. Kettner,[‖] and David A. Agard[*,§]

*Department of Biochemistry and Biophysics and The Howard Hughes Medical Institute,
University of California at San Francisco, San Francisco, California 94143-0448, and Central Research and Development
Department, Experimental Station, E. I. du Pont de Nemours and Company, Inc., Wilmington, Delaware 19898*

Received December 27, 1988; Revised Manuscript Received May 10, 1989

ABSTRACT: To better understand the structural basis of enzyme specificity, the structures of complexes formed between α-lytic protease, an extracellular serine protease of *Lysobacter enzymogenes*, and five inhibitory peptide boronic acids (R_2-boroX, where R_2 is methoxysuccinyl-Ala-Ala-Pro- and boroX is the α-aminoboronic acid analogue of Ala, Val, Ile, Norleu, or Phe) have been studied at high resolution by X-ray crystallography. The enzyme has primary specificity for Ala in the P_1 position of peptide substrates with catalytic efficiency decreasing with increasing side-chain volume. Enzyme affinity for inhibitors with boroVal, boroIle, and boroPhe residues is much higher than expected on the basis of the catalytic efficiencies of homologous substrates. Covalent tetrahedral adducts are formed between the active-site serine and the boronic acid moieties of R_2-boroAla, R_2-boroVal R_2-boroIle, and R_2-boroNorleu. Though R_2-boroVal is a slowly bound inhibitor and R_2-boroAla is rapidly bound [Kettner, C. A., Bone, R., Agard, D. A., & Bachovchin, W. W. (1988) *Biochemistry 27*, 7682–7688], there appear to be no structural differences that could account for slow binding. The removal from solution of 20% more hydrophobic surface on binding accounts for the improved affinity of α-lytic protease for R_2-boroVal relative to R_2-boroAla. The high affinity of the enzyme for R_2-boroIle derives from the selective binding of the L-allo stereoisomer of the boroIle residue, which can avoid bad steric interactions in the binding pocket. While R_2-boroNorleu buries as much hydrophobic surface as R_2-boroVal, its larger side chain causes alterations in enzyme conformation and inhibitor position, leading to a distortion of hydrogen bonds between the enzyme and inhibitor. A trigonal adduct is formed between the active-site serine and the boronic acid moiety of R_2-boroPhe in which the catalytic histidine occupies a position axial to the plane of the trigonal adduct. The histidine $N_{\epsilon 2}$ is 2.2 Å from the boron, suggesting that a coordinate covalent bond has formed.

One of the fundamental functions of an enzyme is to provide specificity by limiting the range of substrates that are catalytically productive. Since catalysis is a result of an enzyme's ability to bind the transition state for a reaction (Wolfenden, 1972), specificity must derive in large part from the selective binding of transition states for the reactions of favored substrates (Fersht, 1977). Studies relating catalytic efficiency to substrate structure serve to identify the important determinants of specificity residing on the substrate (Fersht, 1977). Similarly, site-directed mutagenesis can be used to determine which residues on the enzyme contribute to specificity (Estell et al., 1986). However, a thorough understanding of the interaction of these important structural elements, contributed by both the enzyme and substrate, can only be achieved through direct structural analysis. Of greatest interest are the

structures of enzyme–substrate complexes during the transition state, since determinations of k_{cat}/K_M relate most closely to these structures (Fersht, 1977). While the structure of the transition state itself is inaccessible, the structures of enzyme complexes with analogues of the transition state can be determined. Crystallographic analysis of a series of complexes with systematically varying analogues should provide detailed structural information concerning which interactions are utilized in stabilizing good substrates and which interactions are disrupted with poor substrates. In addition, these structures could be useful as models for other types of molecular recognition such as the binding of ligands by receptors. In this work we report the determination by high-resolution X-ray crystallography of the structures of five enzyme–inhibitor complexes between α-lytic protease and a series of peptide boronic acids varying in the side chain of the boronic acid.

α-Lytic protease is an extracellular serine protease produced by the soil microorganism *Lysobacter enzymogenes*, apparently to bring about the lysis of microbes and small organisms also found in soil (Whitaker, 1970). The enzyme has been extensively studied as a model serine protease largely because it contains a single histidine residue located at the active site, which has facilitated magnetic resonance investigations of the pK_a values of the catalytic residues (Robillard & Schulman,

[*] Author to whom correspondence should be addressed.

[§] University of California at San Francisco.

[‖] E. I. du Pont de Nemours and Co., Inc.

1974; Bachovchin et al., 1981, 1988; Bachovchin & Roberts, 1978; Westler, 1980; Bachovchin, 1986). Kinetic, spectroscopic, and crystallographic evidence suggests that peptide-bond hydrolysis is accomplished via the stabilization of a high-energy tetrahedral intermediate formed by the nucleophilic attack of Ser-195[1] on the carbonyl carbon of the scissile bond (Hunkapiller et al., 1976; Kaplan & Whitaker, 1969; Delbaere et al., 1981; Brayer et al., 1979a,b; Fujinaga et al., 1985; Bone et al., 1987). On small peptide substrates, R_1-X-p-Na,[2] where R_1 is succinyl-Ala-Ala-Pro- and X is Ala, Val, Met, Leu, or Phe, the primary specificity of the enzyme is for Ala in the P_1[3] position with activity falling off dramatically as the size of the P_1 substrate side chain increases (Table I; Delbaere et al., 1981).

Peptide boronic acids, peptide analogues in which the C-terminus (COO⁻) is replaced with $B(OH)_2$, are exceedingly good inhibitors of serine proteases and appear to act by mimicking the formation of high-energy tetrahedral intermediates on the reaction pathway for peptide-bond hydrolysis (Kettner & Shenvi, 1984; Matteson et al., 1981; Bone et al., 1987; Tulinsky & Blevins, 1987; Matthews et al., 1975). Inhibition of α-lytic protease by a series of peptide boronic acids would be expected to improve in parallel with increases in k_{cat}/K_M for a corresponding series of substrates. This is observed for inhibition of the enzyme by a series of peptide-boroVal inhibitors increasing in the number of residues in the peptide (Kettner et al., 1988). However, this is not observed for the inhibition of the enzyme by a series of tetrapeptide boronic acids varying in the side chain of the boronic acid, R_2-boroX, where R_2 is methoxysuccinyl-Ala-Ala-Pro- and boroX is boroAla, boroVal, boroIle, boroNorleu, or boroPhe (see Table I for K_i values). Inhibitors with boroVal, boroIle, or boroPhe are bound much more tightly than would be expected on the basis of the activity of the enzyme toward corresponding substrates. Yet, on the basis of the structure of a complex formed between α-lytic protease and R_3-boroVal, where R_3 is *tert*-butyloxycarbonyl-Ala-Pro-, it appeared that boronic acids are very good analogues of the transition state (Bone et al., 1987).

The inhibitory potency of peptide boronic acids is presumed to derive from their ability to form covalent tetrahedral adducts with the active-site serine residue (Bone et al., 1987; Tulinsky & Blevins, 1987; Matthews et al., 1975). For the most tightly bound inhibitors, corresponding to the best substrates, ^{15}N NMR evidence suggests that tetrahedral adducts are formed with the active-site serine of α-lytic protease (Bachovchin et al., 1988). In contrast, the observation that the enzyme can have high affinity for inhibitors that do not correspond to good substrates indicates that additional factors must be involved in inhibitor binding. It is unknown whether such inhibitors form tetrahedral serine adducts or if the anomalous binding properties of these inhibitors derived from formation of a type of adduct previously unobserved. Alternate adducts that can be formed between the boron and the active-site residues include a trigonal serine adduct, a tetrahedral histidine adduct,

and a tetrahedral adduct in which bonds are formed between the boronic acid boron and both the serine and histidine (Figure 1; Rawn & Lienhard, 1974; Philipp & Bender, 1971). In this regard, Bachovchin et al. (1988) have shown that in the complex with R_2-boroPhe a bond forms between the active-site histidine residue of α-lytic protease and the inhibitor boron.

We have determined the crystal structures of the complexes formed between α-lytic protease and each of the five inhibitors to understand why the enzyme's affinity for these analogues does not parallel values of k_{cat}/K_M for a corresponding series of substrates. Of particular interest was determining the mode of interaction of R_2-boroPhe with α-lytic protease since the benzyl side chain of the boroPhe is much too large to fit into the P_1 binding site. In addition, while R_2-boroAla is bound rapidly by the enzyme, R_2-boroVal is a slow-binding inhibitor. The difference between the fast- and slow-binding inhibitors might also involve the formation of an alternate type of adduct.

EXPERIMENTAL PROCEDURES

α-Lytic protease was purified from culture filtrates of *L. enzymogenes* 495 (ATCC 29487) and migrated as a single band when subjected to low-pH native polyacrylamide gel electrophoresis (Whitaker, 1970; Hunkapiller et al., 1973; Hames & Rickwood, 1981). Crystals of α-lytic protease were grown from 1.3 M lithium sulfate containing Tris–sulfate (20 mM) at ambient temperature (Bone et al., 1987; Brayer et al., 1979b).

R_1-Ala-p-Na, R_1-Met-p-Na, R_1-Leu-p-Na, and R_1-Phe-p-Na were purchased from Bachem Inc. as was methoxysuccinyl-Ala-Ala-Pro-Val-p-Na. Stock solutions of R_1-Val-p-Na were prepared in situ by adding 1.03 equiv of NaOH to a suspension of methoxysuccinyl-Ala-Ala-Pro-Val-p-Na, vortexing vigorously until all of the starting material dissolved, and allowing the reaction to stand for 5 min. Then 0.3 equiv of HCl was added to the reaction to bring the pH to a value of 6 and the solution to volume (0.1 M substrate). Chromatography using an anion-exchange column (Rainin Dynamax 300A 12 μm AX equilibrated with 10 mM Tris–acetate, pH 7.3) showed that the solution contained a single ultraviolet absorbing peak with the same R_f as succinyl-Ala-Pro-Ala-p-Na and no p-nitroaniline or starting material. Values of k_{cat} and K_M for these substrates were determined from double-reciprocal plots of initial reaction velocity as a function of substrate concentration and errors estimated as described by Bevington (1969). Reactions, initiated by the addition of enzyme, contained substrate and 0.1 M Tris-HCl (pH 8.0) and were monitored continuously at 410 nm for the production of p-nitroaniline ($\Delta\epsilon = 8860$ M⁻¹ cm⁻¹; Hunkapiller et al., 1976). For the hydrolysis of R_1-Phe-p-Na, reactions were allowed to progress 16–20 h, and then the absorbance at 410 nm was determined and the initial enzymatic rate of reaction calculated and corrected for the nonenzymatic rate of substrate hydrolysis.

R_2-boroAla, R_2-boroVal, and R_2-boroPhe were synthesized as previously described (Kettner et al., 1988; Kettner & Shenvi, 1984). R_2-boroIle and R_2-boroNorleu were prepared by coupling methoxysuccinyl-Ala-Ala-Pro-OH to H-boroIle-pinacol or H-boroNorleu-pinacol using the mixed-anhydride procedure described previously (Kettner & Shenvi, 1984). H-boroIle-pinacol and H-boroNorleu-pinacol were also prepared by the procedure of Kettner and Shenvi (1984), and the former was kindly provided by A. B. Shenvi. Anal. Calcd for (methoxysuccinyl-Ala-Ala-Pro-boroIle-pinacol) $C_{27}H_{47}N_4O_8B$: C, 57.23; H, 8.38; N, 9.89; B, 1.91. Found: C, 56.90; H, 8.56; N, 9.61; B, 1.86. Anal. Calcd for (me-

---

[1] Residues in α-lytic protease are numbered by homology with chymotrypsin (Fujinaga et al., 1985) and range from 15A to 244.

[2] Abbreviations: R_1, succinyl-Ala-Ala-Pro-; R_2, methoxysuccinyl-Ala-Ala-Pro-; R_3, *tert*-butyloxycarbonyl-Ala-Pro-; MeOSuc-, methoxysuccinyl-; Tris, tris(hydroxymethyl)aminomethane; p-Na, p-nitroaniline; Norleu, norleucine. The prefix "boro" of boroVal- indicates that the carbonyl of the amino acid residues, in this case a valyl residue, is replaced by $B(OH)_2$; the systematic name for valine boronic acid would be (1-amino-3-methylpropyl)boronic acid.

[3] In protease substrate nomenclature the residue to the N-terminal side of the scissile bond is the P_1 residue, the next residue toward the N-terminus is the P_2 residue, etc. (Schecter & Berger, 1967).

Table I: Kinetic Parameters of α-Lytic Protease

substrate	k_{cat}^a (s^{-1})	K_M^a (mM)	k_{cat}/K_M^a (M^{-1} s^{-1})	side-chain vol^b (Å^3)	inhibitor	K_i (nM)
R$_1$-Ala-*p*-Na^c	75 ± 9	3.6 ± 0.4	21000 ± 700	25	R$_2$-boroAla^d	67^e
R$_1$-Val-*p*-Na	13 ± 0.2	16 ± 0.3	790 ± 3	75	R$_2$-boroVal	6.4^e
R$_1$-Met-*p*-Na	56 ± 6	31 ± 3	1800 ± 30	104	R$_2$-boroNorleu	1100
				102	R$_2$-boroIle	40^f
R$_1$-Leu-*p*-Na	1.2 ± 0.9^g	290 ± 230^g	4.2 ± 0.05^g	102		
R$_1$-Phe-*p*-Na	0.0068 ± 0.0007	17 ± 2	0.38 ± 0.01	137	R$_2$-boroPhe	540^e

^{a} Errors were estimated as described by Bevington (1969). ^{b} Values from Chothia (1984). ^{c} R$_1$ is succinyl-Ala-Ala-Pro-. ^{d} R$_2$ is methoxy-succinyl-Ala-Ala-Pro-. ^{e} Values from Kettner et al. (1988). ^{f} Corrected to reflect the relative abundance of D,L-allo-boroIle. ^{g} Values were extrapolated from low substrate concentrations due to substrate inhibition.

thoxysuccinyl-Ala-Ala-Pro-boroNorleu-pinacol) C$_{27}$H$_{47}$N$_4$O$_8$B: C, 57.23; H, 8.38; N, 9.89; B, 1.91. Found: C, 56.13; H, 8.58; N, 9.52; B, 2.11. The K_i values for R$_2$-boroIle and R$_2$-boro-Norleu were determined by the exact procedure described by Kettner et al. (1988). R$_2$-boroIle and R$_2$-boroNorleu were found to be simple competitive inhibitors with K_i values of 81.5 ± 5.4 and 1100 ± 100 nM.

To prepare enzyme–inhibitor complexes, inhibitor solutions (0.1–0.5 M) in water were added in small aliquots (0.25–1.0 μL) to vapor diffusion droplets (5 μL) containing one to three crystals of α-lytic protease. Generally, several aliquots of inhibitor solution were added to the same crystal drop, allowing 24 h of equilibration between additions, to achieve the final inhibitor concentration (Table II). Protease crystals remained undamaged by this procedure except when inhibitors containing boroIle and boroPhe were used. Soaking crystals with these inhibitors resulted in the formation of shallow surface cracks that did not impair diffraction or cause twinning.

Data from crystals of enzyme–inhibitor complexes were collected from single crystals by using either Syntex P21 or Rigaku AFC5R automated diffractometers, equipped with graphite monochrometers (Stroud et al., 1974; Wycoff et al., 1967). For the complexes formed with R$_2$-boroAla, R$_2$-boroVal, R$_2$-boroNorleu, and R$_2$-boroPhe, additional higher resolution data sets were collected from a second crystal and merged with data from the first crystal. Crystals of enzyme–inhibitor complexes were isomorphous with native crystals and generally had cell parameters that differed by less than 0.15%. The complex with R$_2$-boroPhe had *a* and *b* unit cell dimensions 0.5% greater than those of native. The intensities of seven check reflections were monitored to correct for crystal decay, which was less than 20% over the course of data collection. Corrections were also made for absorption, Lorentz, and polarization, by standard methods, and for backgrounds according to the method of Krieger et al. (1974). Data were collected by ω scan in shells of 2θ with the scan rate adjusted so that at least 86% of the reflections had intensities greater than 3σ over the entire data set (Table II).

Initial Fourier maps were computed by using the refined native α-lytic protease coordinates (Fujinaga et al., 1985) with the exception that four water molecules and a sulfate occupying the active site were removed. Maps were inspected and the inhibitors were placed by using the interactive graphics package FRODO (Jones, 1982), after which the coordinates were refined by the stereochemically restrained least-squares algorithm of Hendrickson and Konnert (1981) as adapted for use on the FPS 264 array processor (Furey, 1984) and further modified by us. For the complex with R$_2$-boroPhe a conformational shift required protease residues 162–180 to be refitted into Fourier maps calculated with 2|F$_o$| − |F$_c$| coefficients. The final overall crystallographic *R* factors for the comparison of observed and calculated structure factors are listed in Table II. Surface area calculations (Table II) were done by using the molecular surfacing program MS (Conolly, 1983a,b).

RESULTS

Inhibitor Binding Does Not Parallel Substrate Specificity. Values of k_{cat}, K_M, and k_{cat}/K_M are listed in Table I for the hydrolysis of R$_1$-Ala-*p*-Na, R$_1$-Val-*p*-Na, R$_1$-Met-*p*-Na, R$_1$-Leu-*p*-Na, and R$_1$-Phe-*p*-Na catalyzed by α-lytic protease. Catalytic efficiency falls off as a function of increasing P$_1$ side-chain volume except for R$_1$-Met-*p*-Na, which has the same P$_1$ side-chain volume as R$_1$-Leu-*p*-Na but is enzymatically hydrolyzed at a much higher rate. K_M values increased as a function of P$_1$ side-chain size except for R$_1$-Phe-*p*-Na, which apparently forms a Michaelis complex with the enzyme with the same affinity as R$_1$-Val-*p*-Na. These results demonstrate how strongly the enzyme selects against substrates with large P$_1$ side chains [$(k_{cat}/K_M)_{Ala}/(k_{cat}/K_M)_{Phe}$ = 55 000] but provide no understanding as to how the larger side chains are accommodated by the enzyme active site during the transition state.

Uncertainty regarding the details of enzyme–substrate interactions in the transition state are underscored by the fact that enzyme affinities for peptide boronic acid inhibitors with varying P$_1$ residues do not parallel catalytic efficiencies for homologous substrates (Table I). Most dramatic is the difference between the K_i value of 3.6 mM expected for R$_2$-boroPhe, on the basis of the relative catalytic efficiencies of Ala and Phe substrates and the K_i for R$_2$-boroAla, and the value of 0.54 μM actually observed. This discrepancy is sufficiently large to suggest an alternate mode of binding for the R$_2$-boroPhe inhibitor. In addition, the K_i value for the β-branched boroVal appears anomalously low since Val makes a much poorer P$_1$ substrate than Ala (Table I).

Ala, Val, Ile, Leu, and Norleu Inhibitors Form Tetrahedral Adducts. In addition to the possibility of forming a tetrahedral adduct with the active-site serine residue, boronic acids have the potential to form a trigonal serine adduct, a tetrahedral histidine adduct, or a diadduct in which bonds are formed to both the serine and histidine (Figure 1; Rawn & Lienhard, 1974; Philipp & Bender, 1971). Difference electron density maps clearly showed that all inhibitors (including R$_2$-boroPhe) were bound by the enzyme at a single site with high occupancy. Maps calculated with Fourier coefficients (2|F$_o$| − |F$_c$|) showed continuous electron density stretching between the active-site Ser (195 O$_\gamma$) and the boron of the inhibitors, indicating that in each complex a covalent adduct had formed with the active-site serine. This was corroborated by the bond lengths found on refinement (Table III). On the basis of the shape of the electron density about the boron and bond angles after refinement, the geometry of the adducts, except in the R$_2$-boroPhe complex, were slightly distorted from tetrahedral[4] (Table III).

---

[4] Boron angles of 109° would be expected in a purely tetrahedral adduct, while angles of 120° would be expected in a trigonal planar adduct.
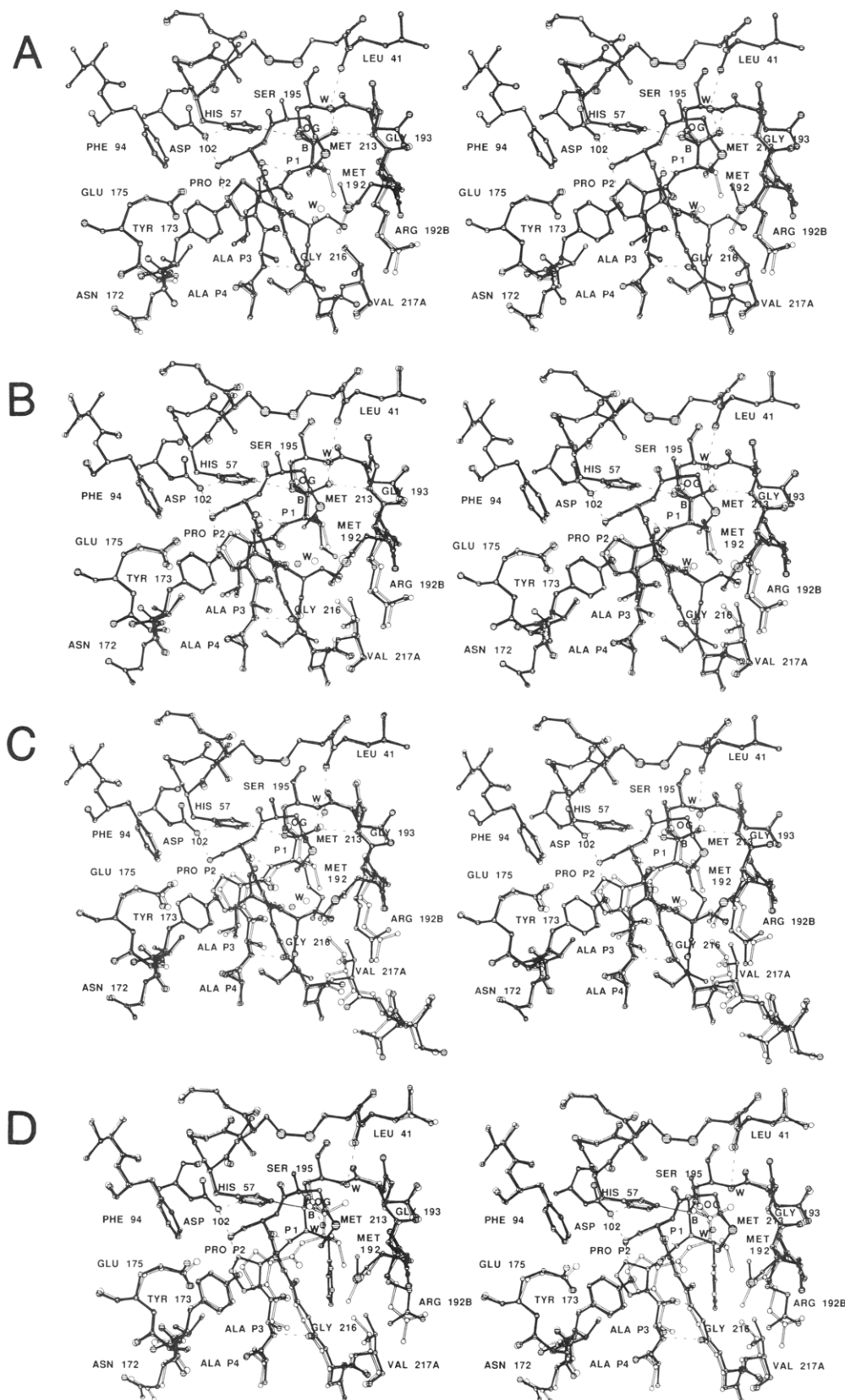
Table II: Crystallography of α-Lytic Protease–Inhibitor Complexes

inhibitor	K_i (nM)	[I] (nM)	resolution (Å)	% rfls, $I > 3\sigma$	R factor	rms deviation from native[a] (Å)	buried surface total (Å^2)	hydrophobic (Å^2)
MeOSuc-Ala-Ala-Pro-boroNorleu	1100	75	2.10	92	0.139	0.15	540	330
MeOSuc-Ala-Ala-Pro-boroPhe	540[b]	25	2.34	86	0.140	0.18	489	280
MeOSuc-Ala-Ala-Pro-boroAla	67[b]	100	2.0	88	0.147	0.12	490	290
MeOSuc-Ala-Ala-Pro-boroIle	40[c]	20	2.55	93	0.134	0.16	550	340
MeOSuc-Ala-Ala-Pro-boroVal	6.4[b]	100	2.15	89	0.142	0.14	540	350

[a] Deviation in C_α coordinates relative to the structure of the unliganded enzyme (Fujinaga et al., 1985). [b] Kettner et al. (1988). [c] This value is corrected for the relative abundance of D,L-allo-boroIle.

FIGURE 1: Four possible structures for boronic acid adducts with a serine protease.

For the tetrahedral adducts, the protein–inhibitor interactions that stabilize the complex are essentially identical with those that stabilize the complex formed between α-lytic protease and R$_3$-boroVal [described in detail in Bone et al. (1987)]. The inhibitors make the same seven hydrogen bonds with the enzyme (three in the oxyanion binding pocket, one with His-57, and three with residues 214–216) and have nearly

the same interatomic distances between hydrogen-bonding atoms (Table III). These inhibitors also make van der Waals contacts with the side chains of Met-192, Met-213, and Val-217A and the main chains of residues 214–216 and 192–193 in the primary specificity pocket (Figures 4 and 5) and with the side chains of Tyr-171, Phe-94, and His-57 in the P$_2$ binding site. No electron density is observed after the P$_4$ Ala residue for any of the inhibitors, indicating that the methoxysuccinyl group is disordered.

Where these four inhibitors do differ is in the way in which the boronic acid side chain fits into, and interacts with, the primary specificity pocket. The primary specificity pocket is composed of the side chains of residues Met-192, Met-213, and Val-217A (Figures 4 and 5), which line the sides of the site, and the main chains of residues 214–216 and 192–193, which cover the bottom and top of the pocket. When a Val side chain is bound in the primary specificity pocket, C_ϵ of Met-192 rotates approximately 120° about the C_γ-S$_\delta$ bond to avoid making a bad contact with $C_{\gamma1}$ of the inhibitor Val. This rotation does not occur when an Ala side chain occupies the site (Figure 3A). The effect of the bond rotation is to allow the Val side chain of R$_2$-boroVal to fit snugly in the P$_1$ binding site and bury 20% more hydrophobic surface upon complex formation than R$_2$-boroAla (Table II; Figure 4A,B). The energy gained from the removal of 60 Å^2 of hydrophobic surface from water (1.5 kcal; Richards, 1977) is sufficient to account for the enhanced affinity of the enzyme for R$_2$-boroVal over R$_2$-boroAla. With the exception of the altered side-chain conformation of Met-192, the two structures are nearly identical (rms deviation in C_α coordinates of 0.07 Å).

By analogy with the amino acid Ile, there are four stereoisomers of boroIle: L-boroIle, D-boroIle, L-allo-boroIle, and D-allo-boroIle; L-boroIle corresponds to naturally occurring Ile. While R$_2$-boroIle is synthesized as a racemic mixture at both chiral centers (C_α and C_β) of the boroIle residue,

FIGURE 2: Stereo drawing of the active site of a 2.55-Å resolution $2|F_o| - |F_c|$ electron density map with positive density contours and the refined model for the complex formed between α-lytic protease and R$_2$-boroPhe. F_c and ϕ_c were calculated from refined coordinates for the enzyme–inhibitor complex.

FIGURE 3: Stereo drawings comparing the structures of α-lytic protease complexes with inhibitory peptide boronic acids. In the drawings are superimposed the structures of the complex with R_2-boroVal in the unfilled bonds and atoms and the complex with R_2-boroAla (A), R_2-boroIle (B), R_2-boroNorleu (C), and R_2-boroPhe (D) in the filled bonds and atoms. Shown are the active-site residues of α-lytic protease, numbered 15A–244 (see footnote 3), including the catalytic triad (Asp-102, His-57, and Ser-195) and the inhibitors, numbered P_4–P_1 (boronic acid residue). Water molecules are labeled W with the water designated 309 located the closest to Leu-41. (A) Note how similar the structures of R_2-boroAla and R_2-boroVal are and the rotation of the terminal methyl group of Met-192 that accommodates the Val side chain of R_2-boroVal. (B) The L-allo isomer of the Ile side chain of R_2-boroIle is bound; there is an adjustment in the position of Val-217A and a slight distortion in the inhibitor chain. (C) In the complex with R_2-boroNorleu note the distortion in the position of the inhibitor (P_4–P_1) and the adjustment in the region of Val-217A. (D) In the complex with R_2-boroPhe a trigonal adduct is formed between the P_1 boroPhe and Ser-195 and a bond to His-57; also note the adjustments in Arg-192B and residues 172–175.
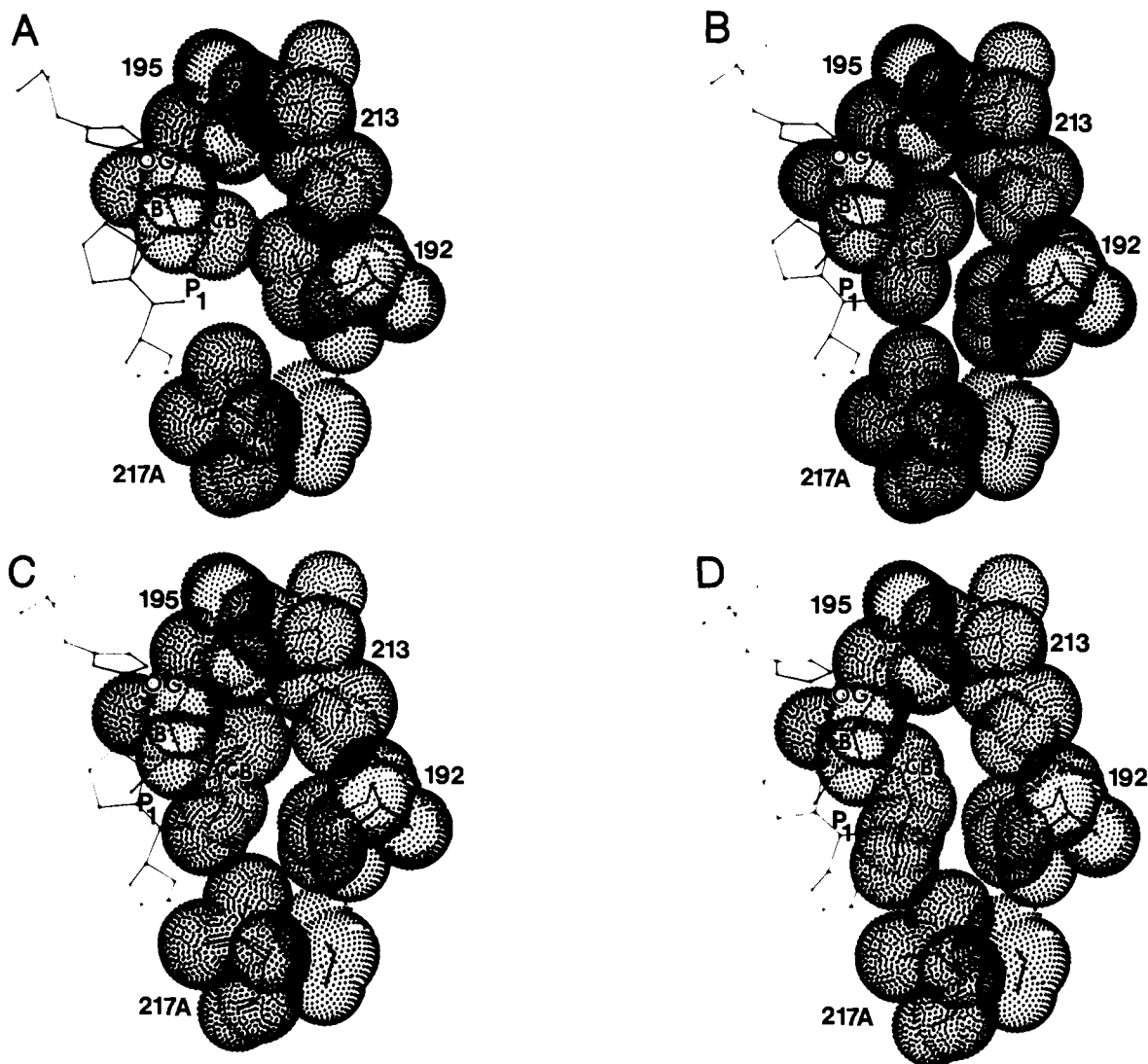
FIGURE 4: Packing efficiency in the specificity pockets of tetrahedral adducts of α-lytic protease with peptide boronic acids. Complexes formed between α-lytic protease and R_2-boroAla (A), R_2-boroVal (B), R_2-boroIle (C), and R_2-boroNorleu (D) are shown. The van der Waals surfaces of the P_1 residue of the inhibitor (center of drawing) and residues 195, 213, 192, 218, and 217A that line the primary specificity pocket of the enzyme (clockwise from top) are displayed. The O_γ of Ser-195 and the B and C_β of the P_1 residue of the inhibitor are labeled. (A) Note packing defects around C_β of the P_1 residue of the R_2-boroAla. (B) Note how efficiently the P_1 side chain of R_2-boroVal fills the specificity pocket. (C) The Ile side chain of the P_1 residue of R_2-boroIle fits almost as well as Val. (D) Packing defects are introduced again when the P_1 Norleu side chain of R_2-boroNorleu projects into the site.

TETRAHEDRAL SER ADDUCT
(R_2-boroAla, R_2-boroVal, R_2-boroIle,R_2-boroNorleu)

TRIGONAL HIS-SER ADDUCT
(R_2-boroPhe)
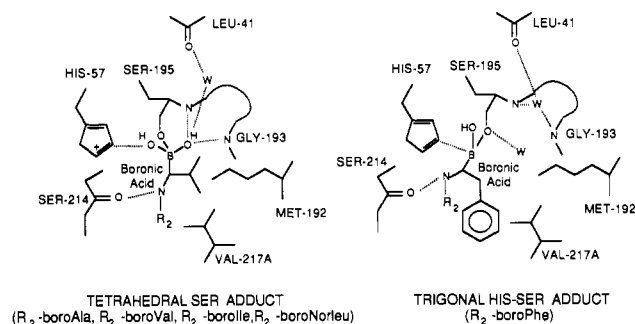
FIGURE 5: Schematic drawing of the interactions that stabilize each of the two types of adduct that have been observed to form in the active site of α-lytic protease.

structural analysis indicates that α-lytic protease preferentially binds R_2-L-allo-boroIle. Since none of the other isomers are observed bound to the enzyme, the enzyme must have at least 5-fold higher affinity for the L-allo isomer (on the basis of a detection limit of 20% occupancy in the Fourier maps). If the stereoisomer corresponding to natural L-Ile was bound by the

enzyme, C_δ of the Ile side chain would be prevented from fitting into the specificity pocket on steric grounds because of the presence of Met-213 and Met-192. By selecting the L-allo stereoisomer, the enzyme binds the inhibitor with the Ile C_δ in a conformation in which it turns back toward the rest of the inhibitor and away from the specificity pocket (Figure 3B). This configuration allows R_2-boroIle to bind in the same manner as R_2-boroVal (Figures 3B and 4) and induces the same small changes in the enzyme including rotation of the terminal methyl group of Met-192. Relative to the structure of the enzyme–R_2-boroVal complex, only a small rotation of the side chain of Val-217A and slight adjustment in the positioning of the inhibitor in the binding site are required for R_2-boroIle to form a complex with the enzyme (rms deviation in C_α coordinates relative to R_2-boroVal = 0.10 Å). However, fit of the Ile side chain of the inhibitor into the P_1 binding site does appear to lead to slight distortion or stretching in some of the hydrogen bonds maintaining the complex (Table III).

Due to the length of its Norleu side chain, R_2-boroNorleu cannot be easily accommodated by the enzyme; consequently, significant conformational shifts occur in the atomic positions

Table III: Bond and Angle Parameters of Inhibitory Complexes

parameter type	parameter	inhibitor					
		R₂-boroAla[a]	R₂-boroVal	R₂-boroIle	R₂-boroNorleu	R₂-boroPhe	R₃-boroVal[b]
bond (Å)	Ser-195 Oγ–boro B[c]	1.61	1.62	1.72	1.64	1.57	1.68
	boro B–boro O₁	1.49	1.51	1.49	1.51	1.42	1.52
	boro B–boro O₂	1.47	1.50	1.47	1.51		1.49
	boro B–boroC_α	1.52	1.53	1.53	1.53	1.53	1.55
	boro B–His-57 N_ε2	3.56	3.53	3.47	3.45	2.18	3.49
hydrogen bond (Å)	Ser-195 N–boro O₁	3.0	3.0	3.0	3.1	4.7	2.9
	Gly-193 N–boro O₁	2.5	2.6	2.7	2.6	5.2	2.6
	wat-309 O–boro O₁	3.2	3.2	3.3	3.6		3.3
	His-57 N_ε2–boro O₂	2.7	2.6	2.8	2.7		2.7
	Ser-214 O–boro N	2.9	3.1	3.0	3.2	3.1	3.0
	Gly-216 N–Ala-P₃O	2.9	2.9	3.0	3.1	3.0	3.0
	Gly-216 O–Ala-P₃N	2.9	3.0	3.1	3.1	3.0	2.9
bond angle (deg)	Ser-195 C_β–Ser-195 Oγ–boro B	136	139	142	129	135	135
	Ser-195 Oγ–boro B–boro O₁	105	100	98	106	110	99
	Ser-195 Oγ–boro B–boro O₂	90	93	101	106		93
	Ser-195 Oγ–boro B–boro C_α	103	105	100	102	120	104
	boro O₁–boro B–boro O₂	115	117	119	115		115
	boro O₁–boro B–boro C_α	121	119	121	118	124	117
	boro O₂–boro B–boro C_α	116	117	111	106		121
	His-57 N_ε2–boro B–Ser-195 Oγ					93	
	His-57 N_ε2–boro B–boro O₁					89	
	His-57 N_ε2–boro B–boro Ca²					109	

[a] R₂ is methoxysuccinyl-Ala-Ala-Pro-. [b] R₃ is *N-tert*-butyloxycarbonyl-Ala-Pro- (Bone et al., 1987). [c] Boro indicates that these atoms are on the boronic acid residue.

of both the enzyme and inhibitor (rms deviation relative to C_α coordinates of R₂-boroVal = 0.13 Å). To accommodate the Norleu side chain of the inhibitor, Val-217A shifts away from the center of the specificity pocket by 0.6 Å, with Val C_γ1 shifting by 1.4 Å (Figure 3C). This shift is attenuated over the next two residues, after which the structure is nearly the same as the structure of the R₂-boroVal complex. Enlargement of the specificity site allows C_ε of the boroNorleu to tuck into the pocket rather than being exposed to solution (Figure 4). However, the Norleu side chain is still too large for the site, and this causes the boronic acid residue itself to move out of the P₁ site by 0.25–0.5 Å toward the P₂ site (Figure 3C). The inhibitor remains tethered to the enzyme by hydrogen bonds between the P₃ Ala residue and the enzyme and between the oxyanion binding site and the boronic acid hydroxyl, though these hydrogen bonds are stretched (Table III). In addition, a weak hydrogen bond between the boronic acid hydroxyl group and a crystallographically ordered water in the oxyanion binding pocket appears to be disrupted in the boroNorleu complex.

R₂-boroPhe Forms a Novel Trigonal Complex. In contrast to the tetrahedral adducts, the geometry of the R₂-boroPhe adduct with α-lytic protease was trigonal planar (Figures 2 and 5). After refinement, His-57 was positioned axial to the adduct with its N_ε2 2.2 Å from the boron, suggesting that a bond had formed between the His nitrogen and the inhibitor boron. The unusual geometry must result because the side chain of R₂-boroPhe is much too large and inflexible to fit into the primary specificity site of the enzyme. This forces the boron atom of the inhibitor away from the oxyanion binding site (residues 193–195) and toward the His-57 (Figure 3D). The inhibitor remains tethered to the enzyme at the P₃ position by the two hydrogen bonds to Gly-216, by a hydrogen bond between the boroPhe amide proton and the carbonyl oxygen of Ser-214, and by covalent bonds to Ser-195 and His-57. The Phe ring of the inhibitor is swung out of the specificity pocket and packs under the aliphatic portion of the side chain of Arg-192B and over the inhibitor Pro. Arg-192B has altered its conformation to optimize the packing of side-chain carbons over the Phe ring and to point its hydrophilic nitrogens away

from the Phe ring and into solution (Figure 3D). One effect of this mode of binding of R₂-boroPhe by the enzyme, with the ring of the inhibitor Phe residue sandwiched between Arg-192B and the inhibitor Pro, is that the active-site cleft must expand. The P₂ Pro of the inhibitor shifts toward the ring of Tyr-171, which in turn adjusts by moving residues 169–175 away from the active site by up to 1.1 Å relative to their positions in the native enzyme (Figure 3D). Residues 169–175 move away from the active site by only 0.5 Å when good inhibitors are bound. These movements are clearly indicated from initial difference Fourier maps and from the positions of these atoms following refinement. In the observed binding mode, R₂-boroPhe buries as much hydrophobic surface area as R₂-boroAla (Table II) but loses three hydrogen bonds in the oxyanion binding pocket (one to an ordered molecule of solvent) and one to His-57.

Average Temperature Factors for the Inhibitors Vary with the Side Chain. Average temperature factors for the inhibitors in these structures appear to correlate with the packing efficiency of the P₁ side chain [average B (Å²) = 17.4, 12.3, 14.6, 15.7, and 18.7, respectively, for R₂-boroX, X = Ala, Val, Ile, Norleu, and Phe]. The R₂-boroVal inhibitor appears to have the most efficient side-chain packing in the specificity pocket since it has the lowest K_i, the most complementary fit to the binding pocket, and enzyme–inhibitor hydrogen bonds nearly equivalent to those of R₂-boroAla. For inhibitors with P₁ side chains that overpack the binding site there is a direct correlation of average inhibitor temperature factor with residue size. The R₂-boroAla inhibitor, which has a significantly smaller P₁ side chain and fails to fill the specificity site, also has a higher average inhibitor temperature factor.

Changes in enzyme temperature factors induced upon complex formation for each of the inhibitors that form tetrahedral adducts parallel alterations observed with the R₃-boroVal complex (Bone et al., 1987), showing significant reduction in the temperature factors for residues 170–175 (ΔB = 10 Å²). In the complex formed between R₂-boroNorleu and the enzyme, the temperature factors for residues 217A–217C are increased by an average of 7 Å² (from average values of 15 Å²). This change is consistent with the shift of these

residues to accommodate the Norleu side chain. Changes in temperature factors resulting from the formation of the R_2-boroPhe complex with α-lytic protease were significantly different from the other complexes. Temperature factors for residues 170–175 that move away from the active site by over 1 Å are increased slightly rather than being decreased as in the other complexes.

DISCUSSION

Inhibitor Binding. On the basis of this structural study the relative binding affinities of the five inhibitors and many aspects of substrate selectivity are now understood. It has been shown that four of the peptide boronic acids, R_2-boroAla, R_2-boroVal, R_2-boroNorleu, and R_2-boroIle, form covalent tetrahedral adducts with the γ oxygen of the active-site serine residue. R_2-boroVal is bound by the enzyme better than R_2-boroAla since it can form the same hydrogen bonds as the weaker complex and also buries 20% more hydrophobic surface area upon complex formation. In addition, the fit of the boroVal side chain into the specificity pocket is very complementary, while the fit of the boroAla side chain leaves gaps (Figure 4A,B), although the energetic consequences of such packing defects are difficult to estimate.

R_2-boroIle is bound very tightly by the enzyme because it exists as a racemic mixture of boroIle stereoisomers from which the enzyme selects the one isomer that can bind tightly, the L-allo isomer. This stereoisomer buries as much surface area as R_2-boroVal (Table II) and makes the same hydrogen bonds. It is bound by the enzyme only a factor of 6 less tightly, apparently because of residual bad contacts in the P_1 binding pocket that subtly distort the geometries of hydrogen bonds holding the enzyme and inhibitor together and because of the loss in configurational entropy due to restraining the conformation of the boroIle side chain.

Interaction of R_2-boroNorleu with α-lytic protease is complicated by a shift in the conformation of the enzyme and by altered positioning of the inhibitor in the active site. The inhibitor buries as much hydrophobic surface upon complex formation as R_2-boroVal, but this is offset by the loss of energy due to formation of poorer hydrogen bonds (Table III), by the diversion of binding energy to drive the conformational shift of the enzyme (Figure 3C), and by the loss of configurational entropy for the highly flexible Norleu side chain. Poorer hydrogen bonds result from the altered positioning of the boronic acid group with relation to His-57 and the oxyanion binding site, which in turn results from the poorer fit of the Norleu side chain in the P_1 binding site.

The formation of a chemically and structurally very different type of adduct explains why R_2-boroPhe binds to α-lytic protease much tighter than expected from the substrate specificity of the enzyme. Of the four boronic acid–serine protease adducts discussed earlier (tetrahedral Ser adduct, tetrahedral His adduct, His-Ser doubly bonded adduct, and trigonal Ser adduct; Figure 1), only the tetrahedral serine adduct had previously been considered a likely possibility. However, when R_2-boroPhe binds to α-lytic protease, a trigonal planar adduct is formed between O_γ of Ser-195 and the boron of the inhibitor in which $N_{\epsilon 2}$ of histidine apparently donates a coordinate covalent bond to boron from an axial position (Figures 3D and 5). This structure for the adduct formed between α-lytic protease and R_2-boroPhe corroborates a recent ^{15}N NMR study of this complex suggesting that either a tetrahedral histidine adduct or an adduct involving bond formation with both His-57 and Ser-195 was formed (Bachovchin et al., 1988). Recently, another group has also observed the formation of

this type of adduct between porcine pancreatic elastase and carbobenzyloxy-Ala-boroIle (Takahashi et al., 1989). Since P_1 Ile substrates are not selected against very strongly by elastase (Harper et al., 1984), steric hindrance would not appear to be the sole driving force behind the formation this unusual adduct.

Though a bond is gained, the R_2-boroPhe complex with α-lytic protease is stabilized by four fewer hydrogen bonds with the active site (two with residues 193–195, one with a water in the oxyanion binding site, and one with His-57) than in the tetrahedral complexes. As much surface area is buried with this complex as in the complex formed with R_2-boroAla. Thus, it seems that the net reduction in binding affinity caused by the loss of these hydrogen bonds and the change in adduct bonding is only a factor of 8 (Table I). In contrast, the loss of just one of the hydrogen bonds between the P_3 residue of the inhibitor and Gly-216 results in a decrease in affinity by a factor of 500 (acetyl-Ala-Pro-boroVal vs acetyl-Pro-boroVal; Kettner et al., 1988; Kettner, unpublished results). Why is the R_2-boroPhe complex so stable despite the loss of hydrogen bonds? One possibility is that the contribution of the histidine–boron coordinate bond may energetically be the equivalent of one or more hydrogen bonds. Alternatively, the trigonal serine adduct might be intrinsically more stable than the tetrahedral adduct. Observation of the tetrahedral adduct with some inhibitors could then be the result of the ability of these inhibitors to take advantage of interactions with the binding pocket that are designed to be optimized during formation of the nearly tetrahedral transition state. As a result of these interactions, the apparent equilibrium constant for adduct formation would be shifted to favor a tetrahedral rather than a trigonal adduct. Although trigonal binding modes are catalytically unproductive, the formation of a trigonal adduct could be exploited in the design of tight-binding inhibitors not on the basis of mechanistic considerations but on the chemical properties of boronic acids and the particular topology of this active site.

Structural Basis for Inhibitor Specificity. Accommodation of side chains in the P_1 binding site of α-lytic protease appears to result in changes in the structure of the enzyme in proportion to the volume of the P_1 side chain of the inhibitor (note the rms deviation of the C_α coordinates of enzyme–inhibitor complexes relative to native α-lytic protease; Table II). Successively larger P_1 side chains in the inhibitors lead to larger shifts in the structure of the enzyme and greater distortion in the positioning of the inhibitor in the active-site cleft (Figure 3A–D). Both effects reduce the binding energy of the inhibitors because some of the potential binding energy is used to alter the structure of the enzyme and because distortions away from the optimal inhibitor position reduce hydrogen-bond energies.

While the accommodation of large side chains by the specificity pocket of α-lytic protease involves significant changes in the structure of the enzyme, there do not appear to be concomitant increases in the effective size of the pocket. The hydrophobic surface area of the inhibitor P_1 side chain that is buried when large side chains interact with the enzyme (50 Å^2 for Ile, Norleu, and Phe side chains) is identical with the amount buried when R_2-boroVal combines with the enzyme. Similarly, the amount of surface area on the enzyme buried when these side chains interact with the specificity site does not improve significantly when side chains larger than Val are bound (Val, 90 Å^2; Ile, 98 Å^2; Norleu, 90 Å^2; Phe, 70 Å^2). Together these observations suggest that the amount of hydrophobic surface the specificity site can bury has remained

constant, despite conformational changes, and that the effective size of the site is unchanged.

Examination of the structures of these enzyme–inhibitor complexes have identified flexible regions of the enzyme that contribute to the P_1 (192B, 217A–217C) and P_2 (170–175) binding sites. These flexible residues appear to have discrete, alternate conformations that are close in energy to their conformations in the unliganded enzyme. Because the energetic penalty for shifting conformations is not too high, inhibitor binding can readily induce these alternate enzyme conformations. Knowledge of such regions of flexibility could be of use in the design of inhibitors since it should be possible to overcome the cost of inducing the conformational shifts by making additional favorable interactions with the enzyme.

Substrate Specificity. The structures of these enzyme–inhibitor complexes were studied as models for enzyme–substrate interactions during the transition state. To the extent that this premise is correct, the manner in which the enzyme interacts with a particular inhibitor is expected to represent how the enzyme binds the transition state for hydrolysis of the corresponding substrate. However, it is clear that at least one aspect of the transition state is not being properly mimicked by these inhibitors. Although R_2-boroVal has a K_i value much lower than that of R_2-boroAla, R_1-Val-*p*-Na is a poorer substrate than R_1-Ala-*p*-Na (Table I). This may derive from the electronic structure of the tetrahedral boronic acid adduct in which negative charge is residing on boron instead of on one of the hydroxyl oxygens as it would be in the authentic reaction intermediate. Perhaps when the tetrahedral intermediate is formed, the oxyanion moves slightly deeper into the oxyanion binding pocket than the neutral hydroxyl group of the boronic acid and improves the hydrogen bond with the amide group of Ser-195 (3.0 Å in inhibitor complexes). Movement of the oxyanion deeper into the oxyanion binding pocket might be prevented in P_1 Val substrates because of steric repulsion between Met-213 and the Val side chain, but not in P_1 Ala substrates (see Figure 4A,B; note packing defects in Figure 4A). Such positioning would be more important for the tetrahedral intermediate, because of the full negative charge on oxygen, than for the boronic acid complex with only a partial negative charge on the hydroxyl. Lengthening of the hydrogen bond to the amide nitrogen of Ser-195 would be reinforced in the boronic acid complexes due to the charge–charge attraction between $N_{\epsilon2}$ of His-57 and the negatively charged boron, which would tend to pull the boron toward His-57 and to move the boronic acid hydroxyl group away from the oxyanion binding pocket. This positioning of boronic acids, resulting from interactions with His-57 and the amide group of Ser-195, could eliminate the steric repulsion between Met-123 and the boroVal side chain that would occur in Val substrates.

Support for this hypothesis can be provided by the increased catalytic efficiency of the enzyme toward R_1-Met-*p*-Na relative to R_1-Val-*p*-Na (Table I) and the mode of binding of R_2-boroNorleu. The high degree of flexibility of a Met side chain would allow it to turn back on itself in the primary specificity pocket in the same manner as the boroNorleu side chain. If a conformation that brings the Met side chain back toward the inhibitor and away from Met-213 were adopted, room would remain in the P_1 binding pocket in the transition state to allow the movement of the oxyanion of the substrate toward the amide group Ser-195 (see Figure 3D). Loss of configurational entropy and residual steric repulsions would be offset by improved oxyanion stabilization and removal of the Met side chain from solvent and would lead to higher catalytic

efficiency than toward R_1-Val-*p*-Na.

The selection against P_1 Leu and Phe substrates derives simply from steric restraints, since these side chains lack the flexibility of a Met side chain; the P_1 Phe substrates are much worse than P_1 Leu substrates because of increased side-chain size. The binding mode of R_2-boroPhe with the Phe ring sandwiched between Arg-192B and the inhibitor Pro may be used by R_1-Phe-*p*-Na to form a Michaelis complex with the enzyme that is as stable as the R_1-Val-*p*-Na Michaelis complex.

Structural Basis for Slow Inhibition. The kinetic mechanism of the slow binding of R_2-boroVal to α-lytic protease involves the rapid formation of a "loose" complex ($K_i = 68$ nM) with subsequent slow conversion to the final "tight" complex ($K_i = 6.4$ nM; Kettner et al., 1988). Other than the rotation of the terminal methyl group of Met-192, there are no structural differences between the R_2-boroVal and R_2-boroAla complexes that could explain why one is slowly bound and the other rapidly bound. It seems unlikely that rotation about a single bond could account for the slow rate of formation of the final complex. The absence of significant differences between fast- and slow-forming complexes of α-lytic protease with boronic acids is similar to the results of another recent study of complexes between thermolysin and phosphoramide peptide analogues (Holden et al., 1987; Bartlett & Marlowe, 1987). In that study, the structure of thermolysin was the same in rapidly and slowly forming complexes, but the inhibitor conformations differed (Holden et al., 1987; Bartlett & Marlowe, 1987). It was proposed that the displacement of an ordered molecule of solvent was responsible for the slow binding of better inhibitors. However, the structures of ordered solvent in complexes of α-lytic protease with rapidly and slowly formed complexes are identical.

Why are the structures of complexes of rapid- and slow-binding boronic acids with α-lytic protease the same? It may be that the crystal lattice forces are sufficient to prevent R_2-boroVal from forming the final tight complex, since the equilibrium constant for conversion to the final complex is only approximately 10. Alternatively, perhaps both slow- and fast-binding inhibitors reach the same final state, but the conversion of the initial complex to the final complex is fast for one inhibitor and slow for the other. For instance, the slowly bound inhibitor might first combine with the enzyme to form one of the other types of adducts (Figures 1 and 5) and then slowly convert into the tetrahedral serine adduct. If this were the case, then the final structures of the two inhibitors would appear the same. However, it might be possible to use low-temperature methods to trap such a transiently formed adduct, thus permitting direct structural analysis by X-ray crystallography.

REFERENCES

Bachovchin, W. W. (1986) *Biochemistry 25*, 7751–7759.
Bachovchin, W. W., & Roberts, J. D. (1978) *J. Am. Chem. Soc. 100*, 8041–8097.
Bachovchin, W. W., Kaiser, R., Richards, J. H., & Roberts, J. D. (1981) *Proc. Natl. Acad. Sci. U.S.A. 78*, 7323–7326.
Bachovchin, W. W., Wong, W. Y. L., Farr-Jones, S., Shenvi, A. B., & Kettner, C. A. (1988) *Biochemistry 27*, 7688.
Bartlett, P. A., & Marlowe, C. K. (1987) *Biochemistry 27*, 8553–8561.

Bevington, P. R. (1969) *Data Reduction and Error Analysis for the Physical Sciences*, pp 92–118, McGraw-Hill, New York.

Bone, R., Shenvi, A. B., Kettner, C. A., & Agard, D. A. (1987) *Biochemistry 27*, 7609–7614.

Brayer, G. D., Delbaere, L. T. J., James, M. N. G., Bauer, C. A., & Thompson, R. C. (1979a) *Proc. Natl. Acad. Sci. U.S.A. 76*, 96–100.

Brayer, G. D., Delbaere, L. T. J., & James, M. N. G. (1979b) *J. Mol. Biol. 131*, 743–775.

Chothia, C. (1984) *Annu. Rev. Biochem. 53*, 537.

Connolly, M. L. (1983a) *J. Appl. Crystallogr. 16*, 548–558.

Connolly, M. L. (1983b) *Science 221*, 709–713.

Delbaere, L. T. J., Brayer, G. D., & James, M. N. G. (1981) *Eur. J. Biochem. 120*, 289–294.

Estell, D. A., Graycar, T. P., Miller, J. V., Powers, D. B., Burnier, J. P., Ng, P. G., & Wells, J. A. (1986) *Science 233*, 659–663.

Fersht, A. (1985) *Enzyme Structure and Mechanism*, 2nd ed., Freeman, San Francisco.

Fujinaga, M., Delbaere, L. T. J., Brayer, G. D., & James, M. N. G. (1985) *J. Mol. Biol. 183*, 479–502.

Furey, W. J. (1984) in *Methods and Applications in Crystallographic Computing* (Hall, S. R., & Ashida, T., Eds.) pp 353–371, Clarendon, Oxford, U.K.

Hames, B. D., & Rickwood, D., Eds. (1981) *Gel Electrophoresis of Proteins*, IRL, Oxford, U.K.

Hendrickson, W. A., & Konnert, J. (1981) in *Biomolecular Structure, Function, Conformation, and Evolution* (Srinivasam, R., Ed.) Vol. 1, pp 43–47, Pergamon, Oxford, U.K.

Holden, H. M., Tronrud, D. E., Monzingo, A. F., Weaver, L. H., & Matthews, B. W. (1987) *Biochemistry 26*, 8542–8553.

Hunkapiller, M. W., Smallcombe, S. H., Whitaker, D. R., & Richards, J. H. (1973) *Biochemistry 12*, 4732–4743.

Hunkapiller, M. W., Forgac, M. D., & Richards, J. H. (1976) *Biochemistry 15*, 5581–5588.

Jones, T. A. (1982) in *Computational Crystallography* (Sayre, D., Ed.) pp 303–317, Oxford University, Oxford, U.K.

Kaplan, H., & Whitaker, D. R. (1969) *Can. J. Biochem. 47*, 305–316.

Kettner, C. A., & Shenvi, A. B. (1984) *J. Biol. Chem. 259*, 15106–15114.

Kettner, C. A., Bone, R., Agard, D. A., & Bachovchin, W. W. (1988) *Biochemistry 27*, 7682–7688.

Krieger, M., Chambers, J. L., Cristoph, G. G., & Stroud, R. M. (1974) *Acta Crystallogr., Sect. A: Phys., Diffr., Theor. Gen. Crystallogr. A30*, 740–748.

Matteson, D. S., Sadhu, K. M., & Lienhard, G. E. (1981) *J. Am. Chem. Soc. 103*, 5241–5242.

Matthews, D. A., Alden, R. A., Birktoft, J. J., Freer, S. T., & Kraut, J. (1975) *J. Biol. Chem. 250*, 7120–7126.

Philipp, M., & Bender, M. L. (1971) *Proc. Natl. Acad. Sci. U.S.A. 68*, 478.

Rawn, J. D., & Lienhard, G. E. (1974) *Biochemistry 13*, 3124–3130.

Richards, F. M. (1977) *Annu. Rev. Biophys. Bioeng. 6*, 151–176.

Robillard, G., & Schulman, R. G. (1974) *J. Mol. Biol. 86*, 541–548.

Schecter, I., & Berger, A. (1967) *Biochem. Biophys. Res. Commun. 27*, 157.

Stroud, R. M., Kieg, L. J., & Dickerson, R. E. (1974) *J. Mol. Biol. 83*, 185.

Takahashi, L. H., Radhakrishnan, R., Rosenfield, R. E., Jr., & Meyer, E. F., Jr. (1989) *Biochemistry* (following paper in this issue).

Tulinsky, A., & Blevins, R. A. (1987) *J. Biol. Chem. 262*, 7737–7743.

Westler, W. M. (1980) Ph.D. Dissertation, Purdue University, West Lafayette, IN.

Whitaker, D. R. (1970) *Methods Enzymol. 19*, 599–613.

Wolfenden, R. (1972) *Acc. Chem. Res. 5*, 10–18.

Wycoff, H. W., Dorscher, R., Tsernoglou, D., Inagami, T., Johnson, L., Hrdman, K. D., Allewell, N. M., Kelly, D. M., & Richards, F. M. (1967) *J. Mol. Biol. 27*, 563–578.